The Journal of Korean Vacuum Science & Technology
Vol. 3, No. 2, October 1999, pp. 139~144

Hydrogen concentration and critical epitaxial thicknesses in low-temperature Si(001) layers grown by UHV ion-beam sputter deposition

Nae-Eung Lee

School of Metallurgical and Materials Engineering, Sungkyunkwan University
300 Chunchun-dong, Suwon 440-746, Korea

(Received August 13, 1999)

Abstract – Hydrogen concentration depth profiles in homoepitaxial Si(001) films grown from hyperthermal Si beams generated by ultrahigh vacuum (UHV) ion-beam sputtering have been measured by nuclear reaction analyses as a function of film growth temperature and deposition rate. Bulk H concentrations C_H in the crystalline Si layers were found to be below detection limits, $\approx 1 \times 10^{19}$ cm^{-3}, with no indication of significant H surface segregation at the crystalline/amorphous interface region. This is quite different than the case for growth by molecular-beam epitaxy (MBE) where strong surface segregation was observed for similar deposition conditions with average C_H values of $\approx 5 \times 10^{19}$ cm^{-3} in the crystalline/amorphous interface region and $\approx 10^{20}$ cm^{-3} in the amorphous overlayer. The markedly decreased H concentrations in the present experiments are due primarily to hydrogen desorption by incident hyperthermal Si atoms. Reduced H surface coverages during growth combined with collisionally-induced filling of interisland trenches and enhanced interlayer mass transport provide an increase in critical epitaxial thicknesses by up to an order of magnitude over previous MBE results.

I. Introduction

It has become well established over the past several years that high-structural-quality epitaxial semiconductor layers can be grown at temperatures well below those previously thought to be minimum values [1-4]. Critical epitaxial thicknesses t_e ranging from 7 nm at $T_s = 150$°C to 120 nm at 300°C for Si(001) growth by molecular-beam epitaxy (MBE) with $R_{Si} = 0.07$ nm-s^{-1} [1] have been reported. The use of energetic hyperthermal Si beams increases t_e substantially [4]. In all cases, however, continued growth of epitaxial Si(001) or Ge(001) at low-temperatures leads to an increasingly rough surface with a locally abrupt non-reversible transition to amorphous-layer deposition.

The primary models proposed to explain epitaxial breakdown involve kinetic surface roughening [2, 5-7] and impurity segregation [2, 8-9]. Interlayer transport clearly plays a decisive role in determining surface roughening and the extent of epitaxy during multilayer growth [6, 7]. Eaglesham [2] pointed out that explaining the observed relatively rapid crystalline to amorphous transition based upon kinetic roughening during epitaxial growth in the two-dimensional (2D) multilayer mode requires a roughening exponent β (where the surface width w varies with film thickness t as $w \propto t^{\beta}$) greater than 0.5. Recent *in-situ* scanning tunneling microscopy (STM) roughening studies of low-temperature (LT) homoeptiaxial MBE Ge(001) yield a roughness exponent of order of unity [6]. Lee *et al.*, [7] using atomic force microscopy (AFM) to determine the surface morphological evolution of low-temperature Si(001) during film growth using hyperthermal Si atoms, reported β values ranging from 0.6 for epitaxial layers with $t < t_e$ to 1.3 at thicknesses near epitaxial breakdown.

The presence of impurities such as H [2, 8, 9] and Sb [10] has been shown to decrease t_e for MBE and ion-beam sputter deposited LT Si, respectively. Pre-adsorbed H coverages of $\cong$1 ML on Si(001) substrates inhibits epitaxy and degrades the quality of as-deposited epitaxial layers [11, 12]. Intentional H dosing at 2×10^{-2} ML-s^{-1} during MBE Si(001) growth at $T_s = 310$°C and R = 0.1 nm-s^{-1} decreased t_e from 100 nm to 20 nm [9]. Indirect evidence for H surface segregation affecting t_e is also provided

by experiments showing that repetitive rapid thermal annealing (RTA) above the monohydride desorption temperature (≈515°C) [13], prior to reaching t_e, extends epitaxial growth [8]. Nuclear reaction analysis (NRA) measurements carried out on MBE *Si(001) films deposited at* $T_s = 220°C$ *with* $R = 0.02$ nm-s^{-1}, followed by a 150 s RTA at 450°C (below the monohydride desorption temperature), showed that bulk H concentrations incorporated from the ambient background during film growth were $\approx 2\times10^{20}$ cm^{-3}. However, C_H decreased to $\approx 3\times10^{19}$ cm^{-3} following a 150 s RTA at 650°C [8]. Even the presence of small dopant concentrations during low-temperature Si(001) epitaxy also has been shown to decrease t_e. Sb doping with $C_{Sb} = 2\times10^{18}$ cm^{-3} during LT Si(001) growth at 0.1 nm-s^{-1} reduced t_e by approximately a factor of two over the growth temperature range T_s = 250-300°C [10].

In this work, the concentration of unintentinally incorporated hydrogen in the films was measured in order to investigate the epitaxial breakdown mechanisms in the present experiments. The film growth experiments were carried out as a function of T_s (80-300°C) and R_{Si} (0.008-0.1 nm-s^{-1}). Hydrogen concentration depth profiles and t_e were determined by NRA and cross-sectional transmission electron microscopy (XTEM), respectively.

II. Experimental procedure

All film growth experiments were conducted in a three-chamber load-locked ultra-high vacuum (UHV) system [14, 15]. The growth chamber is cryo-pumped with a base pressure of $\approx 1\times10^{-10}$ Torr and contains facilities for *in-situ* reflection high-energy electron diffraction (RHEED) and residual gas analysis. The ion-pumped analytical chamber is equipped with an Auger electron spectrometer (AES). Sputtering is carried out using a UHV double-grid multi-aperture broad ion-beam source with provisions for *in-situ* spatial adjustment [14]. High purity hyperthermal Si beams, with average energies $\langle E_{Si} \rangle \cong 18$ eV per atom [15], were generated by bombarding a 10-cm-diameter undoped float-zone Si(001) wafer using a 1 keV ultra-high-purity Kr^+ *ion beam. The design of the system geometry, single-crystal Si apertures, and the use of higher mass* Kr^+ ions, rather than Ar^+, minimized kinetic-energy transfer to the growth surface from backscattered ions. Incorporated metallic impurity concentrations were below secondary ion mass spectrometry detection limits (1×10^{15}-10^{16} cm^{-3}). The presence of four hot W filaments (two in the ion gun, one in an ion *gauge, and one in the substrate heater) during deposition* should result in atomic H fluxes at the film growth surface which are at least of the order of those experienced during Si MBE.

The substrates used in these experiments were nominally-singular Si(001)2×1 wafers with miscut of 0.16° toward [110] as measured by high-resolution x-ray diffraction corresponding to an average terrace width of 50 nm. Substrate preparation consisted of degreasing followed by a UV ozone treatment, H passivation in dilute HF, degassing in UHV at 200°C for 1 h, hydrogen desorption at 650°C for 10 s, and the growth of 100-nm-thick Si buffer layers at 650°C in order to obtain comparably smooth starting surfaces with nearly equal root-mean-square surface widths ≈0.07 nm, as determined by atomic force microscopy measurements. TEM and XTEM analyses of as-deposited films were performed using Philips CM-12 and Hitachi 9000 microscopes operated at 120 and 300 kV, respectively. Average total epitaxial thicknesses t_e, defined as the midpoint of the transition (i.e., the average position of the fluctuating crystalline/amorphous interface) were determined from *XTEM micrographs using observations* from more than 20 different regions in each sample.

C_H depth profiles were measured by the ^{15}N nuclear resonance analysis (NRA) method, in which the yield of characteristic γ-rays created through the resonance reaction

$$^{15}N + H \rightarrow {}^{12}C + {}^{4}He + \gamma\text{-ray (4.43 MeV)} \qquad (1)$$

is proportional to the H concentration [16]. The reaction cross-section at the ^{15}N resonance energy of 6.385 MeV is four orders of magnitude larger than the off-resonance cross-section. Thus, H depth profiles can be obtained by varying the incident ^{15}N energy, whose range in the present experiments is 6.3-7.0 MeV. The hydrogen detection limit is $\approx 1\times10^{19}$ cm^{-3} with a depth resolution of ≈100 Å.

III. Results and discussion

Figure 1 shows typical H depth profiles from LT

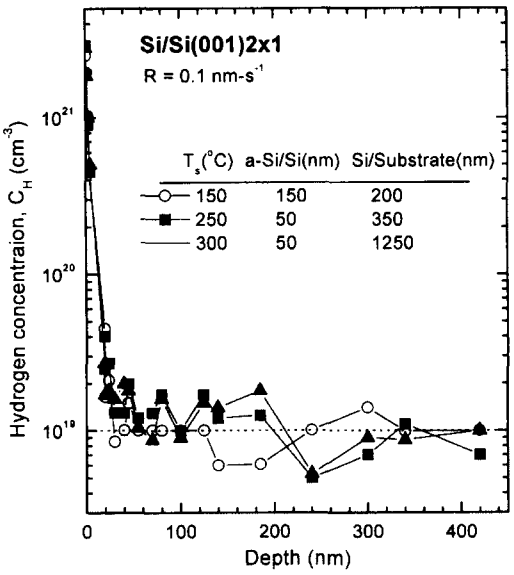

Fig. 1. Typical H depth profiles through Si(001) epitaxial films grown from hyperthermal beams to a thickness past epitaxial breakdown. The deposition rate R was 0.1 nm-s^{-1}.

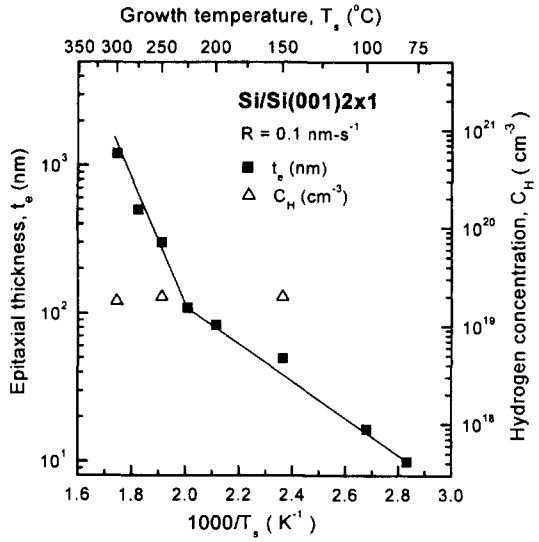

Fig. 2. Critical epitaxial thicknesses t_e of Si(001) epitaxial films grown as a function of T_s using $\langle E_{Si} \rangle \cong 18$ eV Si beams. Bulk hydrogen concentrations C_H in the amorphous overlayers are also plotted. The deposition rate R was 0.1 nm-s^{-1}.

Si(001) layers grown at different substrate temperatures with $R_{Si} = 0.1$ nm-s^{-1} together with the positions of the amorphous/crystalline and the crystalline/substrate interface. The total film thickness is larger than the critical epitaxial thickness t_e and the upper sublayer is amorphous. The high H concentrations observed at all sample surfaces are the result of air-exposure and primarily attributable to adsorbed H_2O. C_H decreases rapidly with sample depth to a value of $\approx 1.5\times10^{19}$ cm^{-3}, just larger than the detection limit, in the amorphous overlayer before falling below the background level, 1×10^{19} cm^{-3}, in the epitaxial layer. There is no indication of excess H accumulation at the crystalline/amorphous interface region as was reported for secondary ion mass spectrometry (SIMS) depth profiles through LT MBE Si(001) layers [9]. In the latter case, the authors interpreted the H accumulation at the crystalline/amorphous (c/a) interface region as an indication of H surface segregation leading to significant surface coverages during LT Si(001) epitaxy. Previous NRA profiles of LT MBE Si(001) layers grown at 220°C with $t < t_e$ also show evidence for H surface segregation and, moreover, the LT epitaxial layers contain rather large H concentrations, $C_H \cong 2.5\times10^{20}$ cm^{-3} [8].

H accumulation at the c/a interface region during LT MBE occurs due to the combination of H surface segregation during growth of the epitaxial sublayer and interface trapping since the H incorporation probability is substantially higher in the amorphous than in the epitaxial sublayer [9]. Based upon our results showing C_H less than detection limits, 1×10^{19} cm^{-3}, with no evidence for H surface segregation, we conclude that H surface coverages in the present hyperthermal beam experiments remain low during epitaxial growth. Rather than H accumulation at the c/a interface, we find that C_H increases gradually from a value less than the detection limit in the epitaxial sublayer to a constant value just above the detection limit in the amorphous sublayer. The nature of this gradual increase is due to the statistical nature of kinetic roughening (see discussion in refs. 5-7) giving rise to a transition zone thickness Δt over which the layers evolve from being fully epitaxial to fully amorphous. Δt in the present experiments is ≈30-35% of the total epitaxial thickness t_e, consistent with what has been reported for LT MBE Si [1] and Ge [3].

Measured C_H values in the amorphous sublayers

are plotted in Fig. 2 together with epitaxial thicknesses t_e obtained from LT hyperthermal Si(001) films grown as a function of T_s (75 to 300°C) with a constant deposition rate, R = 0.1 nm-s^{-1}. There is clearly no correlation between C_H and t_e. Critical thicknesses in the present experiments range from 50 to 1200 nm while the steady state H concentration in the amorphous sublayers remains essentially constant at $\approx 1.5\times10^{19}$ cm^{-3}. These results should be compared to the MBE case in which, with very similar film growth rates, t_e is up to an order of magnitude smaller [1] while C_H, as measured by NRA, was more than an order of magnitude larger [8]. The large increase in t_e observed for low-temperature Si(001) film growth from hyperthermal compared to thermal beams has previously been attributed primarily to collisional effects leading to continuous filling of interisland trenches formed during 2D multilayer growth [4]. A decrease in the slope of $\ln(t_e)$ vs $-1/T_s$ at $T_s < 225$°C was explained in terms of changes in average island sizes giving rise to corresponding changes in interlayer mass transport [4].

The present results suggest that the incident hyperthermal Si atoms play an additional role during film growth in collisionally desorbing surface H, thus maintaining low steady-state surface coverages and bulk H concentrations. Previous molecular-dynamic simulations gave a threshold energy for collisionally-induced H desorption from Si(001) by incident energetic Si particles of ≈7.4 eV [17] and a yield of ≈0.2 for 15 eV Si [18, 19]. Although quantitative prediction is difficult to be made because, depending upon impact parameters, forward scattering and recoil trapping of H atom in the lattice are also possible, it is nevertheless clear that LT Si(001) growth by hyperthermal Si beams with an average kinetic energy $\langle E_{Si} \rangle \cong 18$ eV/atom can give rise to collisionally-induced desorption of surface H. The relatively low H concentrations in our amorphous sublayers provide further evidence for the efficiency of this effect and are consistent with previous results reported for low-energy ion-irradiation-induced H desorption during reactive magnetron sputter deposition of amorphous Si:H [20].

All the previous observations of epitaxial breakdown in LT Si(001) and Ge(001), whether grown by MBE [1, 3] or from hyperthermal beams [4], exhibit a direct correlation with surface roughening [5-7]. That is, low- and high-resolution XTEM micrographs of crystalline/amorphous interface regions in all three cases are essentially identical even though t_e values vary by up to an order of magnitude. The same is true for the growth of LT Si(001):Sb [10]. Even though steady-state Sb surface coverages of only 4×10^{-5} ML during film growth reduced t_e by a factor of two, the Sb had no apparent effect on the surface morphology at epitaxial breakdown. Similarly, the dramatic increase in film roughening rates observed during LT Si(001) homoepitaxy on 4° toward [100] and [110] miscut substrates resulted in corresponding decreases in critical epitaxial thicknesses [7]. Thus, the data suggests that, at least for covalent semiconductors, epitaxial breakdown is directly related to the surface roughness and anything that affects the roughening rate -- e.g., contamination, surface vicinality, substrate material, etc. -- affects the critical thickness accordingly.

The above argument suggests that the primary role of low coverages of surface H atom during LT Si(001) and Ge(001) growth is to inhibit adatom diffusivity as has been shown both experimentally [21], and through first principles total energy calculations [22, 23], for Si(001) homoepitaxy. Lower adatom migration velocities lead to reduced mean free paths which thereby increase the surface roughening rate by augmenting the island nucleation rate on terraces and, hence, causing a more rapid progression to 2D multilayer growth. This, in turn, leads directly to a decrease in t_e. The important point to note, however, is that the presence of surface H accelerates epitaxial breakdown through an indirect route, the inhibition of adatom mobilities, rather than being a direct cause of breakdown.

As a final test of the above hypotheses, we vary another kinetic parameter, the film deposition rate R, during LT hyperthermal-beam Si(001) film growth at constant T_s. The deposition temperature was maintained at 150°C, in the lowest temperature regime shown in Fig. 1, with R ranging from 0.008 to 0.1 nm-s^{-1}. Initial decrease in R from 0.1 to 0.06 nm-s^{-1} results in t_e increasing from 50 to 80 nm. This, we ascribe to increased adatom diffusion lengths at lower R values giving rise to higher step crossing probabilities and decreased surface roughness. Zhang and Lagally [24] predicted that the surface roughness should vary as $R^{0.5}$. However,

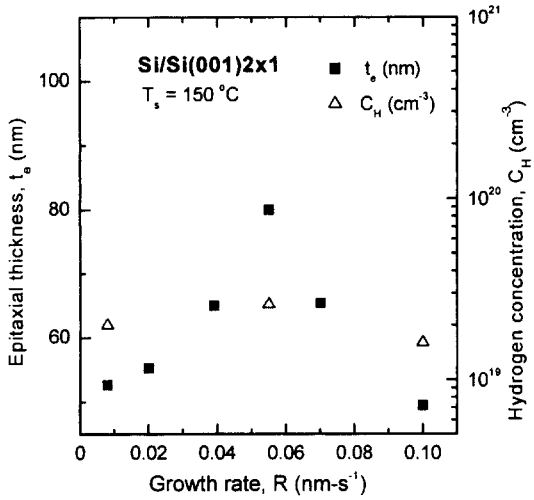

Fig. 3. Critical epitaxial thicknesses t_c of Si(001) epitaxial films grown as a function of the deposition rate R using $\langle E_{Si} \rangle \cong 18$ eV Si beams. Bulk hydrogen concentrations C_H in the amorphous overlayers are also plotted. The growth temperature T_s was 150°C.

decreasing R at constant T_s also leads to larger adatom mean free paths and, hence, increased island sizes which, as discussed above, tends to increase surface roughness. Thus, t_c in the experiments summarized in Fig. 3 is determined by the competition between these two kinetic processes resulting in a maximum in t_c vs R. The most important point to note, however, is that even though t_c varies strongly with R_{Si}, C_H in the amorphous sublayer remains approximately constant at $\approx 1.5 \times 10^{19}$ cm^{-3} (Fig. 3) while it is below the detection limit in the epitaxial sublayers. NRA H depth profiles from these samples are very similar to those shown in Fig. 1 with no indication of H accumulation in the crystalline/amorphous interface region. Thus, there is again no evidence that H surface coverage during low-temperature epitaxial growth is the rate limiting step for epitaxial breakdown.

IV. Conclusions

The results show that bulk H concentrations C_H in the epitaxial layers were below detection limits, $\approx 1 \times 10^{19}$ cm^{-3}. Even in the amorphous overlayer, C_H was $\leq 2 \times 10^{19}$ cm^{-3}. The absence of measurable H accumulation at the crystalline/amorphous interface region indicates that there was no significant H surface coverage during growth of the epitaxial sublayer. Finally, although critical epitaxial thickness values were factors of 5-10 higher than previous MBE results [1, 2], we did not observe any correlation between C_H and t_c. We attribute the low H concentrations in the present layers, compared to reported values for MBE Si(001) films [1, 2], as being due to hyperthermal-irradiation-induced hydrogen desorption during film growth. These results demonstrate that adsorption, surface segregation, and build-up of a critical H surface concentration is not the rate limiting step, in general, for epitaxial breakdown. Rather, epitaxial breakdown occurs even in the absence of significant H coverages. Any process -- including the use of hyperthermal beams, surface contamination, and substrate miscut -- which changes the rate of surface roughening, affects t_c disproportionately.

Acknowledgements

This paper was supported by SEOK CHUN Research Fund, Sunkyunkwan University, 1998. He also thanks Professor J. E. Greene at the University of Illinois at Urbana-Champaign, USA and Björgvin Hjörvarsson at Royal Institute of Technology, Sweden for providing samples and help in H concentration measurements, respectively.

References

1. D. J. Eaglesham, H.-J. Gossmann, and M. Cerullo, *Phys. Rev. Lett.* **65**, 1227 (1990).
2. D. J. Eaglesham, *J. Appl. Phys.* **77**, 3597 (1995).
3. G. Xue, H. Z. Xiao, M.-A. Hasan, J. E. Greene, and H. K. Birnbaum, *J. Appl. Phys.* **74**, 2512 (1993).
4. N.-E. Lee, G. A. Tomasch, and J. E. Greene, *Appl. Phys. Lett.* **65**, 3236 (1994).
5. D. J. Eaglesham and G. H. Gilmer, in *Surface Disordering: Growth, Roughening and Phase Transitions*, edited by R. Jullien, J. Kertesz, P. Meakin, and D. E. Wolf (Nova, New York, 1993), p. 69.
6. J. E. Van Nostrand, S. J. Chey, M.-A. Hasan, D. G. Cahill, and J. E. Greene, *Phys. Rev. Lett.* **74**, 1127 (1995).
7. N.-E. Lee, David G. Cahill, and J. E. Greene, *Phys. Rev.* B **53**, 7876 (1996).
8. P. Asoka-Kumar, S. Szpala, B. Nielson, Cs. Szeles, K. G. Lynn, W. A. Lanford, C. A. Shepard, and H.-J. Gossmann, *Phys. Rev.* B **51**, 4630 (1995).

9. D. J. Eaglesham, F. C. Unterwald, H. Luftman, D. P. Adams, and S. M. Yalisove, *J. Appl. Phys.* **74**, 6615 (1993).
10. N.-E. Lee and J. E. Greene, *Appl. Phys. Lett.* **67**, 2459 (1995).
11. M. Copel and R. M. Tromp, *Phys. Rev. Lett.* **72**, 1236 (1994).
12. S. H. Wolff, S. Wagner, J. C. Bean, R. Hull, and J. M. Gibson, *Appl. Phys. Lett.* **55**, 2017 (1989).
13. H. Kim, G. Glass, T. Spila, N. Taylor, S.Y. Park, J.R. Abelson, and J.E. Greene, *J. Appl. Phys.* **82**, 2288 (1997).
14. G. A. Tomasch, Y.-W. Kim, L. C. Markert, N.-E. Lee, and J. E. Greene, *Thin Solid Films* **223**, 212 (1993).
15. N.-E. Lee, G. Xue, and J. E. Greene, *J. Appl. Phys.* **80**, 769 (1996).
16. W. A. Lanford, *Nucl. Instrum. Methods Phys. Res.* B **66**, 65 (1992).
17. M. V. Ramana Murty and Harry A. Atwater, *Surf. Sci.* **374**, 283 (1997).
18. M. V. Ramana Murty and Harry A. Atwater, *Nucl. Instrum. Methods Phys. Res.* B **102**, 293 (1995).
19. M. E. Taylor, Harry A. Atwater, and M. V. Ramana Murty, *Thin Solid Films* **324**, 85 (1998).
20. J. R. Abelson, L. Mandrell, and J. R. Doyle, *J. Appl. Phys.* **76**, 1856 (1994).
21. J. E. Vasek, Z Zhang, C. T. Salling, and M. G. Lagally, *Phys. Rev.* B **79**, 17207 (1995).
22. J. Nara, T. Sasaki, and T. Ohno, *Phys. Rev. Lett.* **79**, 4421 (1997).
23. S. Jeong and A. Oshiyama, *Phys. Rev. Lett.* **79**, 4425 (1997).
24. Z. Zhang and M. G. Lagally, *Phys. Rev. Lett.* **72**, 693 (1994).